Human Molecular Genetics, 2003, Vol. 12, No. 13 1543–1554
DOI: 10.1093/hmg/ddg170

Targeted inactivation of dystrophin gene product Dp71: phenotypic impact in mouse retina

Cécile Dalloz[1,†], Rachel Sarig[2,†], Patrice Fort[1,†], David Yaffe[2], Agnès Bordais[1], Thomas Pannicke[3], Jens Grosche[3], Dominique Mornet[4], Andreas Reichenbach[3], José Sahel[1], Uri Nudel[2] and Alvaro Rendon[1,*]

[1]INSERM U-592, Laboratoire de Physiopathologie Cellulaire et Moléculaire de la Rétine, Hôpital Saint-Antoine, Bâtiment Kourilsky, 6ème étage, 184 rue du Faubourg Saint-Antoine, 75571 Paris Cedex 12, France, [2]Department of Molecular Cell Biology, Weizmann Institute of Science, Rehovot 76100, Israel, [3]Paul Flechsig Institute for Brain Research, Leipzig University, 04109 Leipzig, Germany and [4]INSERM U 128, Institut Bouisson Bertrand, Montpellier, France

Received March 3, 2003; Revised April 23, 2003; Accepted May 5, 2003

The abnormal retinal neurotransmission observed in Duchenne muscular dystrophy (DMD) patients and in some genotypes of mice lacking dystrophin has been attributed to altered expression of short products of the dystrophin gene. We have investigated the potential role of Dp71, the most abundant C-terminal dystrophin gene product, in retinal electrophysiology. Comparison of the scotopic electroretinograms (ERG) between Dp71-null mice and wild-type (wt) littermates revealed a normal ERG in Dp71-null mice with no significant changes of the b-wave amplitude and kinetics. Analysis of DMD gene products, utrophin and dystrophin-associated proteins (DAPs), showed that Dp71 and utrophin were localized around the blood vessels, in the ganglion cell layer (GCL), and the inner limiting membrane (ILM). Dp71 deficiency was accompanied by an increased level of utrophin and decreased level of β-dystroglycan localized in the ILM, without any apparent effect on the other DAPs. Dp71 deficiency was also associated with an impaired clustering of two Müller glial cell proteins—the inwardly rectifying potassium channel Kir4.1 and the water pore aquaporin 4 (AQP4). Immunostaining of both proteins decreased around blood vessels and in the ILM of Dp71-null mice, suggesting that Dp71 plays a role in the clustering and/or stabilization of the two proteins. AQP4 and Kir4.1 may also be involved in the regulation of the ischemic process. We found that a transient ischemia resulted in a greater damage in the GCL of mice lacking Dp71 than in wt mice. This finding points at a crucial role played by Dp71 in retinal function.

INTRODUCTION

Dystrophin was first described as a large protein of 427 kDa, with partial amino acid sequence homology to the spectrin family of membrane cytoskeletal proteins (1). It consists of four structural domains: (i) an N-terminal actin-binding region with homology to α-actinin; (ii) a rod structure with 24 spectrin-like repeats; (iii) a cysteine-rich domain with calcium-binding motives; and (iv) a unique C-terminal domain. The cysteine-rich and C-terminal domains interact with the plasma membrane via a glycoprotein complex (2,3). Dystrophin is normally present under the sarcolemma of the skeletal muscle as a part of a large protein complex, which forms a linkage between the cytoskeleton, the sarcolemma, and the extracellular matrix (4). It was suggested that it is also involved in the clustering of voltage-gated sodium channels, NO synthase and AQP4 (5–7).

The defective expression of muscle dystrophin results in Duchenne muscular dystrophy (DMD), an X-linked genetic disease characterized by progressive muscle degeneration, leading to death (8). Dystrophin isoforms are also expressed in cardiac and smooth muscle (9) and, at lower levels, in the brain (10). In addition to the full-length dystrophin isoforms, activation of several internal promoters of the DMD gene controls the production of developmentally regulated short products named Dp260 (11), Dp140 (12), Dp116 (13) and

*To whom correspondence should be addressed. Tel: +33 149284604; Fax: +33 149284605; Email: rendon@st-antoine.inserm.fr
†The authors wish it to be known that, in their opinion, the first three authors should be regarded as joint First Authors.

Dp71 (14–16), in reference to their respective molecular weights. Both full-length dystrophin isoforms and the short products are expressed in the nervous system, including brain and retina, where they have a selective distribution within specific brain regions and retinal layers (17–19).

Non-muscular manifestations of DMD have also been described, including cognitive impairments and an abnormal retinal electrophysiology. The abnormal electroretinogram is the best characterized of all the non-muscular manifestations of DMD. Analysis of the dark-adapted (scotopic) electroretinogram (ERG) revealed a reduction in the amplitude of the b-wave response in 80% of DMD patients, as well as in the dystrophic mouse mdx^{3cv} (20,21). Studies of the scotopic ERGs recorded in DMD patients and in X-linked muscular dystrophy mouse strains manifest a genotype–phenotype correlation, based on the DMD gene products affected by the mutation (22–26). DMD patients with normal ERGs usually display mutations located 5′ of the initiation site of Dp260 transcript. Patients with more distal mutations predominantly show an abnormal ERG. This suggests that Dp260 is primarily involved in the generation of the b-wave, and that Dp71 expression is not sufficient to maintain a normal b-wave when dystrophin, Dp260 and Dp140 are missing (27). However, in mdx mouse strains, the genotype–phenotype correlation seems to be somewhat different. In mdx strains with mutations at the 5′ end of the gene (mdx and mdx^{5cv}) which affect only dystrophin, normal ERGs were recorded. Mice with mutations in the middle of the gene, affecting either dystrophin and Dp260 (mdx^{2cv}) or dystrophin, Dp260 and Dp140 (mice lacking exon 52 of the dystrophin gene and mdx^{4cv}), show an increased implicit time of the b-wave but no significant reduction in its amplitude (24,25). The mdx^{3cv} strain has a mutation close to the 3′ end of the dystrophin gene, affecting all the DMD gene products; the ERGs of such mice show both increased implicit time and attenuation of the b-wave amplitude (21). The ERG phenotypes of the mouse strains mentioned above are compatible with a possible involvement of the three DMD gene short products, Dp260, Dp140 and Dp71, in retinal electrophysiology.

Müller cells are the major glial cell type of the retina. They are thought to play a major role in keeping the homeostasis of the retina, particularly of potassium ions, H^+ ions and glutamate. The potassium flux predominantly occurs via the inwardly rectifying potassium channels, Kir4.1. In Müller glial cells from rat retina, Kir4.1 channels are colocalized with the water channel AQP4, which is thought to be responsible for the control of (trans-) retinal water transport (28). Thus, the two proteins together may play a key role in K^+ and water balance, processes that are challenged in many instances of retinal injury including ischemia. Moreover, the Müller cell-mediated potassium currents have been suggested to participate in the generation of the b-wave (29) although this view was recently questioned, as similar b-waves amplitudes were recorded in ERGs of young Kir4.1$^{+/+}$ and Kir4.1$^{-/-}$ mice (30). It is noteworthy that significantly reduced b-wave potentials were observed in AQP4-null mice (31).

Dp71 consists of a unique seven-residues N-terminus fused to the cysteine-rich and C-terminal domains of dystrophin (16,32). It is the major product of the DMD gene in the central nervous system (32). In the mouse retina, Dp71 is localized around retinal blood vessels and at the ILM (33,34). In the rat retina this protein is expressed in Müller glial cells, and is involved in a protein complex including β-dystroglycan, δ-sarcoglycan, α-dystrobrevin and α1-syntrophin (35,36). It has been proposed that this complex could be responsible for the clustering of AQP4 and Kir4.1 in specific membrane areas of the Müller cells (36).

To elucidate the role(s) of Dp71 in the retina, we used a Dp71-null mouse strain in which Dp71 expression was specifically inactivated by homologous recombination, without interfering with the expression of other products of the DMD gene (33). ERG analysis of Dp71-null mice and their wt littermates revealed no significant change in b-wave implicit time and amplitude. Using X-gal staining and immunohistochemistry, we substantiated the localization of Dp71 at the GCL, at the ILM and around the blood vessels, and that of Dp427, Dp260 and Dp140 in the outer plexiform layer (OPL). Experiments with cultured Müller cells showed that murine Müller cells expressed only Dp71 and utrophin. We found that the absence of Dp71 resulted in reduced levels of β-dystroglycan at the inner limiting membrane (ILM). Other DAPs tested were not affected. We also found a change in the localization of Kir4.1 and AQP4 in Müller cells. Western blot analysis revealed that the AQP4 level was markedly reduced in the retinae lacking Dp71 whereas the level of Kir4.1 was not affected. Finally, we found that, as a consequence of absence of Dp71, the ganglion cells were more susceptible to damage resulting from transient ischemia. This finding provides a direct evidence for an essential role of Dp71 in Müller cells.

RESULTS

Electroretinography of Dp71-null mice

In order to determine whether Dp71 is involved in retinal electrophysiology, we compared the scotopic ERGs of Dp71-null mice to those of wt littermates. Representative ERGs are shown in Figure 1. Table 1 includes the mean ERG implicit times, amplitudes, b/a-wave ratios, and the results of Student's t-test. This analysis revealed normal a-wave implicit times and b-wave amplitudes and kinetics, but slightly reduced a-wave amplitude in the ERGs of Dp71-null mice. However, there was no significant difference in the b/a-wave ratio between the two strains.

The levels of Dp140 and utrophin are elevated in the retina of Dp71-null mice

To study the expression of the dystrophin gene products, retinae extracts were examined by immunoblotting using 2166, an antibody that recognizes all DMD gene products (37). This analysis revealed the presence of four bands corresponding to full-length dystrophin, Dp260, Dp140 and Dp71 in the wild-type extracts (Fig. 2A, lane 1). As expected, the Dp71-specific band was not detected in extracts from Dp71-null mice. Both dystrophin (Dp427) and Dp260 were present without changes in their expression level, while Dp140 was elevated in Dp71-null mice (Fig. 2A, lane 2). The blot was also stained with an anti-utrophin-specific antibody. The level of utrophin was increased in Dp71-null mice as compared to the wt mice (Fig. 2B, lanes 1 and 2). These results suggest an, at least

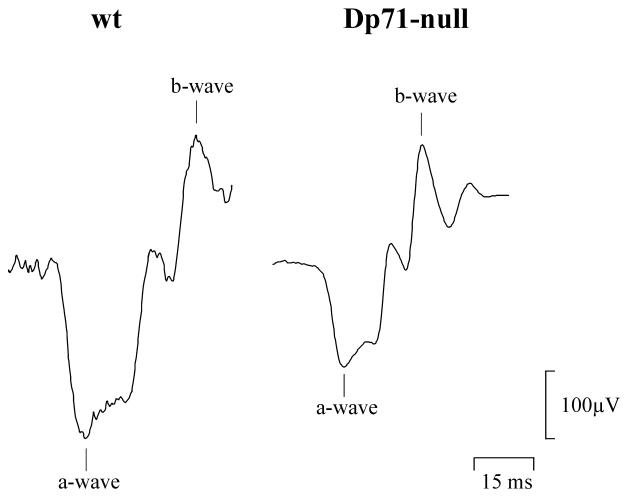

Figure 1. Representative Ganzfeld electroretinograms recorded with full frequencies from wild-type littermates (wt; left) and Dp71-null mice (right). Implicit times (ms) were measured from the stimulus marker to the peak for the a-waves and b-waves, respectively. The b-wave amplitude and kinetics in mice from Dp71-null strain were indistinguishable from those of wt strain; however, the Dp71-null mice showed a significant decrease of the a-wave amplitude.

Table 1. Electroretinographic findings in wild-type and mutant mice

	Wild-type (littermates) (n = 13)	Dp71-null (n = 11)	P-value
Amplitude (μV)			
a-wave	203 ± 11.47	163 ± 10.41	0.0180*
b-wave	381 ± 17.32	348 ± 23.02	0.2603
b/a ratio	1.91 ± 0.091	2.11 ± 0.093	0.1406
Implicit time (ms)			
a-wave	8.54 ± 0.45	8.89 ± 0.38	0.5642
b-wave	32.77 ± 1.35	32.07 ± 1.74	0.752

The values are mean ± SEM at stimulus intensity of 10 cd/m^2.
*$P < 0.05$.

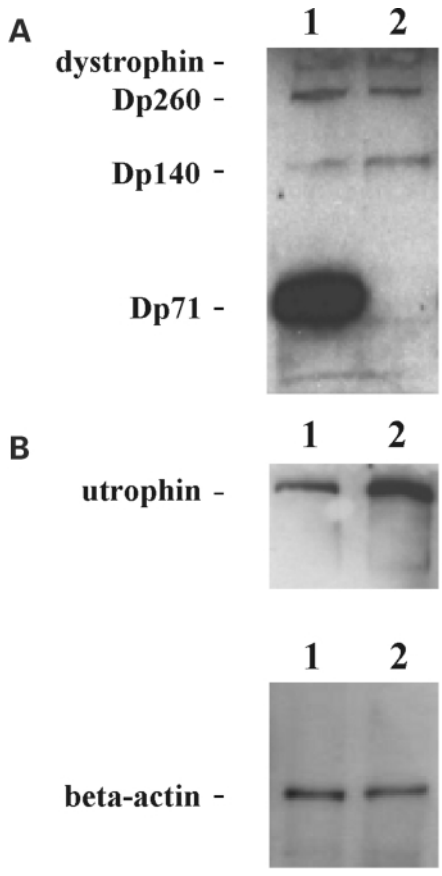

Figure 2. Identification of DMD gene products (A) and utrophin (B) in the murine retina. Western blot of extracts from retinae of wild-type littermates (1) and Dp71-null (2) mice were stained with the polyclonal antibodies 2166 (A) and K7 (B). The full-length dystrophin, Dp260, Dp140 and Dp71 (lane 1) were detected; as expected, the band at 71 kDa (lane 2) is not present in Dp71-null mice (A). Utrophin level is increased (lane 2) in Dp71-null retina as compared to the wild-type (lane 1) (B). β-Actin was used as a loading control.

partial, compensation for the missing Dp71 by utrophin and Dp140.

Localization of DMD gene products

In order to characterize the cellular pattern of expression of Dp71, we performed X-gal staining on retinae from Dp71-null mice in which the endogenous promoter of Dp71 drives β-galactosidase expression (33). We previously showed that, during embryonic development (at 13.5 dpc, days post coitum), the inner layers of the developing retina were β-gal positive.

At this stage, the differentiated layers of the mature retina are not yet developed (33). Staining of adult retinal slices (1–3 month old mice) revealed the expression of β-gal at the ILM, at the ganglion cell layer (GCL) and in a subset of cells at the inner nuclear layer (INL), compatible with an expression of Dp71 in the Müller (glial) cells (Fig. 3A and C) as previously reported for rat retina (36).

Serial retinal sections from Dp71-null mice and their wt littermates were used to determine the localization of DMD and utrophin gene products. The exon 78-specific dystrophin antibody, Dys2, revealed a punctuate signal in the OPL and a staining around the blood vessels in the retina of wild-type mice. We also observed a signal at the ILM (Fig. 4A). In Dp71-null retina, only the OPL signal was evident (Fig. 4B). These observations further confirm the localization of Dp71 at the ILM and around the blood vessels. Other DMD gene products such as dystrophin, Dp260 and Dp140 were localized at the OPL. A possible low-level expression of these proteins in other cell layers cannot be excluded.

Immunostaining with the K7 antibody is shown in Figure 4C and D; this antibody recognizes exclusively utrophin gene products. In contrast to Dys2, the K7 immunolabel did not involve a punctuate staining in the OPL of wild-type retinae; rather, the signal was localized around the blood vessels and at the ILM. In the Dp71-null retinae, the labeling intensity at the ILM and around blood vessels was even increased. This suggested that both utrophin and Dp71 were present at the ILM, possibly in the Müller cell endfeet. To elucidate this point, we studied the mRNA levels of each of the DMD gene products and of utrophin in Müller cell cultures obtained from

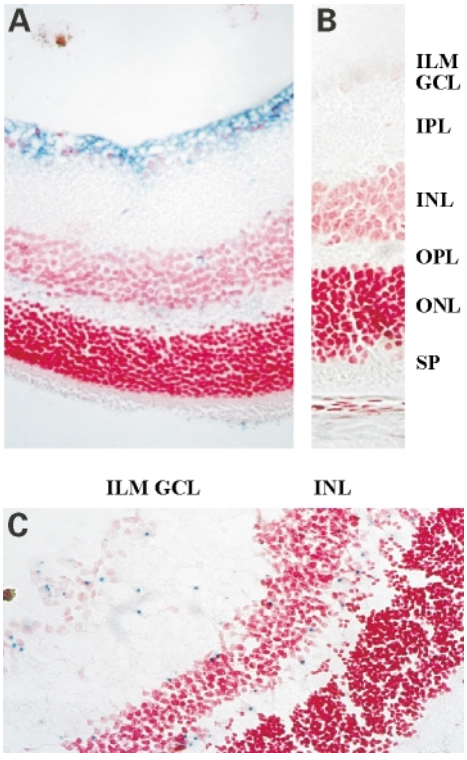

Figure 3. Dp71 promoter activity in the retina of adult mice. Eyes from Dp71-null mice were fixed in 4% PFA, stained with X-gal, dehydrated, embedded in paraffin and cut on a microtome. The slices were deparaffinized with xylene, rehydrated, counterstained with nuclear fast red, dehydrated again and mounted with entellan. Staining was observed mainly at the ILM-GCL (A). Control staining of a wild-type retina (B). In order to exclude the possibility of insufficient penetration of the staining solution, eyes were cut with a cryostat, and the slices were stained with X-gal (C). In addition to the ILM-GCL, staining was then also observed in the INL. ILM, inner limiting membrane; GCL, ganglion cell layer; IPL, inner plexiform layer; INL, inner nuclear layer; OPL, outer plexiform layer; ONL, outer nuclear layer; SP, segments of photoreceptors.

wt and Dp71-null mice. We found that cultured normal Müller cells express both Dp71 and utrophin but no other DMD gene products. In cells from Dp71-null mice, we did not detect any Dp71 mRNA; there was no apparent difference in the utrophin transcript level if compared to the wild strain (unpublished data). However, western-blot analysis and immunostaining showed that the level of utrophin was higher in the retinae of Dp71-null mice than in the retinae of wt mice (Fig 2B).

DAPs in the retina of Dp71-null mice

Previous reports have shown that the loss of dystrophin gene products results in a concomitant loss of members of the DAPs complex from the cell membrane in muscle and brain (38,39 and our unpublished observation). In the retina of mdx^{3cv} mice, in which the levels of all the DMD gene products are greatly reduced, the level of β-dystroglycan was decreased at the OPL (40). To investigate whether the absence of Dp71 alone has an effect on the levels and/or the localization of members of the DAPs complex, we immunostained retinal sections from wt and from Dp71-null mice with anti-DAPs antibodies. The anti β-dystroglycan antibody, JAF, clearly demonstrated the

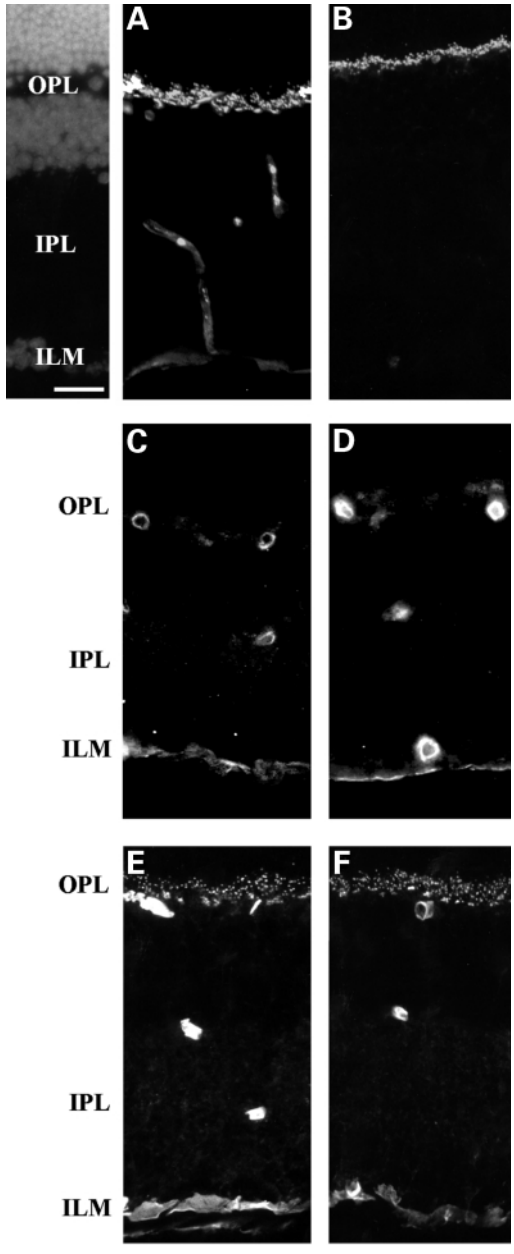

Figure 4. Immunohistochemistry of retinae from wild-type littermate (A, C, E) and Dp71-null (B, D, F) with antibodies against DMD gene products (A, B), utrophin gene products (C, D) and β-dystroglycan (E, F). Immunoreactivity with the Dys2 antibody revealed a signal at the ILM and around the blood vessels in wild-type retina (A), which was absent in the Dp71-null mice (B), while the signal observed at the OPL persisted. With a specific antibody against utrophin gene products, the staining obtained around blood vessels and at the ILM in wild-type retina (C) was markedly increased in the Dp71-null mice (D). The staining with β-dystroglycan antibody decreased at the ILM from Dp71-null mice (F). Top left side: the nuclear layers in a section of the same field were stained with DAPI. Scale bar, 25 μm.

localization of β-dystroglycan in the OPL, at the ILM, and around blood vessels in retinal sections from wild-type mice (Fig. 4E) as reported previously (34,40–43). The signal at the ILM was reduced in retinal sections from Dp71-null mice, while the labeling appeared normal at the OPL and around the

blood vessels (Fig. 4F). This suggests that Dp71 is involved in the stabilization of β-dystroglycan at the ILM. It is quite likely that the remaining β-dystroglycan is stabilized by forming a complex with utrophin, which is up-regulated in the retina of Dp71-null mice (Fig. 2B).

It has been previously demonstrated in the rat retina that β-dystroglycan interacts with δ-sarcoglycan, and that the signaling protein, α1-syntrophin, is able to form a complex with Dp71 and/or utrophin (36). Using antibodies directed against δ- and γ-sarcoglycan and against α1-syntrophin, we found that the levels and localizations of these DAPs in the retina were not affected by the absence of Dp71 (unpublished data), thus suggesting the existence of a complex with other proteins than Dp71, probably with utrophin.

Altered distribution of Kir4.1 and AQP4 in Dp71-null mice

It has been hypothesized that in rat Müller cells the DAPs complex may participate in the clustering of channel proteins such as the potassium channel, Kir4.1, and the water channel, AQP4, via an interaction with PSD-93 (36). We performed immunohistochemical staining of retinal slices, in order to evaluate the effect of the absence of Dp71 on the localization of these channel proteins. In wild-type retinae, double immunolabeling with the anti-Kir4.1 and the anti-vimentin antibodies (44) shows strongly stained vimentin-positive Müller cells spanning the whole thickness of the retina from the outer limiting membrane (OLM) to the ILM (Fig. 5A–D) as previously reported (30). Clustering of Kir4.1 was detected in the endfoot region and around blood vessels (Fig. 5C, arrowheads). A considerable overlap of the vimentin- and Kir4.1-staining patterns was observed close to the ILM, confirming the expression of both proteins in Müller cells. In Dp71-null retinae, the localization pattern of vimentin was not changed (Fig. 5B). However, the Kir4.1 immunolabel was reduced at the ILM as well as around blood vessels (Fig. 5D, arrowheads). A rather diffuse 'overall staining' of Müller cells for Kir4.1 was observed in the retinae of Dp71-null mice.

Previous studies in retina revealed nearly identical patterns of AQP4 and Kir4.1 immunofluorescence (28). We therefore investigated whether the absence of Dp71 may have also altered the AQP4 distribution. Similar to what was found in the rat retina, in wild-type mice the pattern of staining by the anti-AQP4 antibody was only slightly different from that for Kir4.1. Both immunoreactivities were enriched at the endfeet and around blood vessels (Fig. 5I, arrowheads). The only conspicuous difference was noted within the inner plexiform layer (IPL) where only a weak and diffuse AQP4 staining of the Müller cell fibers was detected. In Dp71-null retina, we observed a dramatic diminution of the AQP4 label around the blood vessels and a slight but distinct reduction at the ILM (Fig. 5J, arrowheads). Thus, as in the case of Kir4.1, Dp71 may be involved in the clustering of the water channel, AQP4, in specialized areas of Müller cell membrane.

AQP4 level is reduced in the retinae of Dp71-null mice

If the levels of Kir4.1 and AQP4 in the retina of Dp71-null mice were compared with those in the retina of normal mice by western blotting, we found that the level of Kir4.1 did not change but that the level of AQP4 was greatly reduced in Dp71-null mice (Fig. 6). These results suggest that the perturbed localization patterns of Kir4.1 and AQP4, caused by the absence of Dp71, may be generated by different molecular mechanisms that trigger, in the Müller cells, a specific reduction of the protein content of AQP4 but not of Kir4.1. It is also possible that, when AQP4 is not localized properly, it is less stable than Kir4.1.

Electrophysiological recordings of K^+ currents in dissociated Müller cells

In order to test whether the redistribution of the Kir4.1 channels modifies the electrophysiological properties of Müller cells, whole-cell recordings were made on dissociated cells. Fifteen Müller cells from two Dp71-null mice and 13 cells from three wild-type mice were investigated. The 'resting membrane potential' (zero current potential) of the cells from Dp71-null mice was -86 ± 2 mV. These values were not significantly different from those found in wild-type mice (-88 ± 4 mV). The membrane resistance was recorded in the same cells by applying a 10 mV hyperpolarizing step from the holding potential of -80 mV; it amounted to 24 ± 6 MΩ in cells from Dp71-null mice and to 32 ± 14 MΩ in wild-type cells. Again, this difference was not statistically significant. Hyper- and depolarizing voltage steps between -180 and 0 mV were applied from a holding potential of -80 mV, and the whole-cell K^+ currents were measured. These experiments revealed that the overall K^+ conductances were virtually unchanged in Müller cells from Dp71-null mice, as compared to those from wt mice (Fig. 7A and B).

Membrane potential and membrane resistance depend critically on the functional expression of Kir channels (45) that can be blocked by application of Ba^{2+}. We found that in the presence of 1 mM Ba^{2+}, the membrane potential decreased significantly to -51 ± 8 mV in cells from Dp71-null mice and to -45 ± 7 mV in wt cells; the membrane resistance increased significantly to 752 ± 275 MΩ and 911 ± 496 MΩ, respectively (the differences between Dp71 null-mice and wt were not significant). As shown in Figure 7C and D, a large part of the membrane currents was blocked by Ba^{2+} in cells from both groups of mice, demonstrating that currents through Kir channels are the dominating current type in these murine Müller cells. It can be concluded that while the absence of Dp71 affects the clustering of the channel protein Kir4.1 in specialized regions of the Müller cell membrane, it does not seem to affect the overall level and/or the opening probability of the channel protein.

Ischemia sensitivity of ganglion cells in Dp71-null mice

An elevation of the extracellular glutamate concentration is known to be an important factor in the neuronal damage associated with retinal ischemia. Retinal glutamate homeostasis may be impaired by a loss of the normal accumulation of Kir4.1 in the endfoot membrane, as (i) effective retinal K^+ siphoning requires high Kir4.1 channel densities in Müller cell endfeet, (ii) increased extracellular K^+ depolarizes the Müller cell membrane, and (iii) depolarization reduces the driving

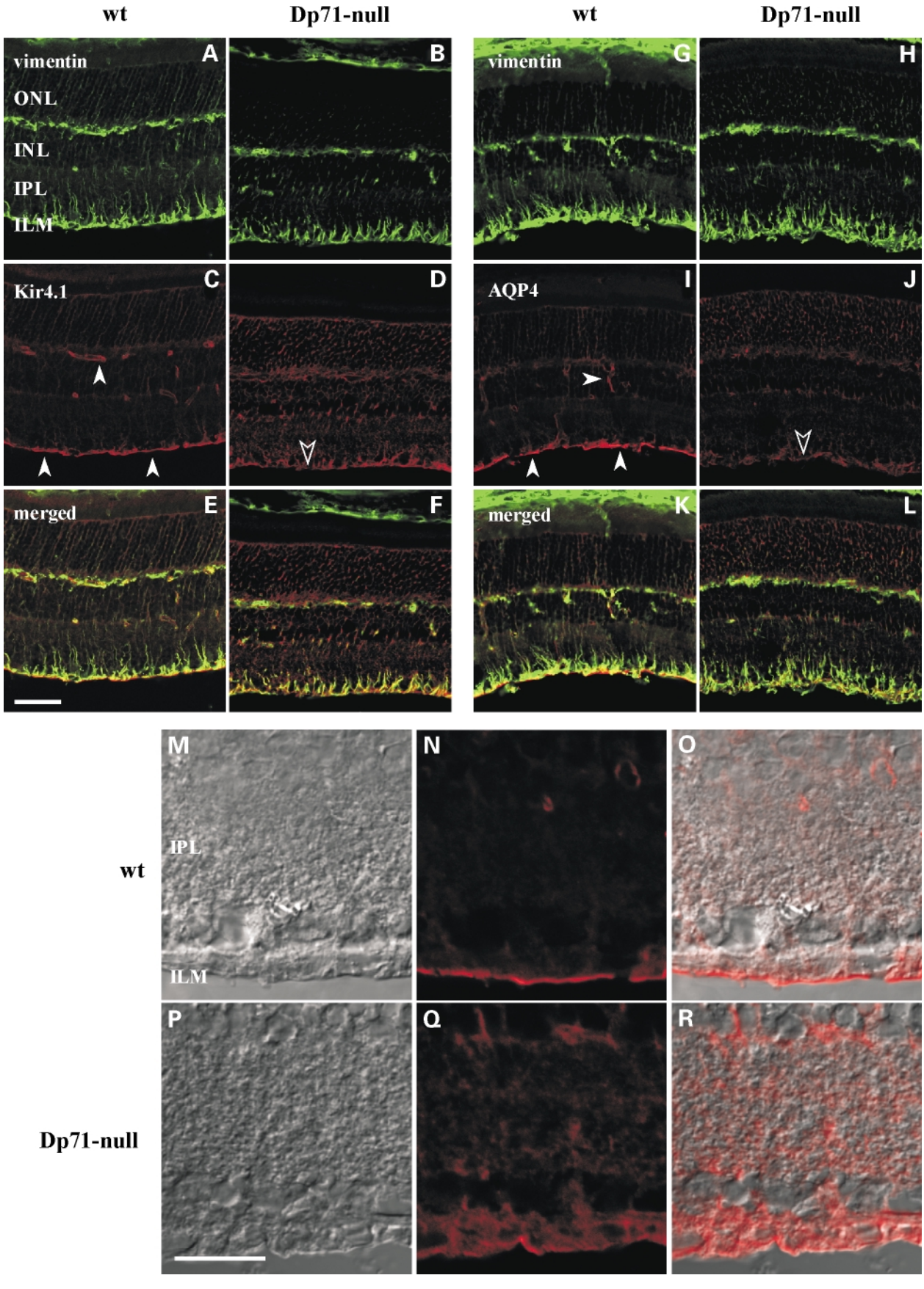

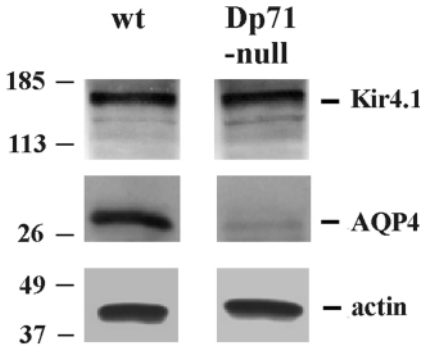

Figure 6. Analysis of Kir4.1 and AQP4 protein level in total retina from wild-type littermates (wt) and Dp71-null mice. Kir4.1 antibody recognizes a main band at ~160 kDa corresponding to its tetrameric form and AQP4 antibody shows a predominant band at ~30 kDa. In Dp71-null retina as compared to the wt, AQP4 level is dramatically decreased, whereas Kir4.1 level doesn't show distinguishable difference. β-Actin was used as a loading control.

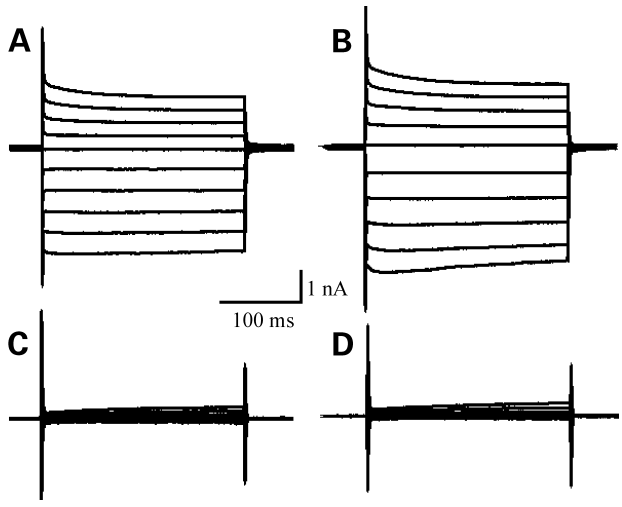

Figure 7. Membrane currents of murine Müller cells. Membrane currents in a Müller cell from a Dp71-null mouse (A) were evoked by voltage steps between −180 and 0 mV from a holding potential of −80 mV (20 mV increment). The current pattern was very similar to that found in a Müller cell from a wild-type littermate (B). To demonstrate that a large part of the membrane currents flows through inwardly rectifying K^+ channels, we applied Ba^{2+} (1 mM), a well-known blocker of these channels. Under these conditions (C, Dp71-null; D, wild-type), the inward currents evoked by hyperpolarizing steps were completely blocked and the outward currents at depolarizing potentials were largely reduced in both cells. Under Ba^{2+}, the cells were only hyperpolarized up to −140 mV.

force for the electrogenic glutamate uptake carriers of Müller cells (cf. 'Discussion' section). Thus, we tested the susceptibility of Dp71-null mice to retinal transient ischemia. Fifteen days after pressure-induced ischemia, the retinae of both control and Dp71-null mice were compared with the non-ischemic eyes of both groups of animals. As shown in Figure 8A, in all animals the retinae subjected to transient ischemia/reperfusion were reduced in thickness (particularly the inner retinal layers) and showed a decreased density of retinal ganglion cells. However, these changes were more pronounced in the ischemia-treated retinae of the Dp71 null-mice. In these retinae, even the layered structure of the retina (inner plexiform and inner nuclear layers) became disorganized at some places (Fig. 8A). We also observed that the decrease of the retinal ganglion cell density was significantly greater in Dp71-null mice (75%) than in wt mice (−50%; Fig. 8B). These data suggest that Dp71 plays an important role in the processes which prevent ganglion cell damage caused by ischemia.

DISCUSSION

Electrophysiology of the retina and of the Müller cells

The ERG is a recording of the sum electrical signal generated by the retina in response to light. Despite of intense research in the field over many years, the underlying mechanisms and the relevant cellular interactions are still not fully elucidated. In particular, the mechanism of the generation of the b-wave is controversial. The b-wave has been attributed to ON-bipolar cell currents (46), to secondary potassium fluxes through Müller cells (mediated by the Kir4.1 K^+ channel) (29,49,50), and to current loops in bipolar (and amacrine) cells (51–54). Recently, the earlier-suggested contribution of Müller cell-mediated K^+ currents to the generation of the b-wave was seriously questioned, as virtually normal b-wave amplitudes were recorded in the ERGs of young mice lacking Kir4.1 (30).

The abnormal ERG of DMD patients is quite unique, as it is not accompanied by any visual disturbances (27,47,48). It has been suggested that, in DMD patients, the abnormal ERG is associated with mutations that disrupt the synthesis of dystrophin and of Dp260. The situation is different in mice, in which the loss of dystrophin, Dp260 and Dp140 is not sufficient to induce a reduction of the b-wave amplitude (although an increased implicit time of the b-wave has been reported) (21,24). Here we demonstrate that the selective loss of Dp71 does not cause a b-wave reduction. These observations suggest that in mice the concomitant lack of dystrophin, Dp260, Dp140 and Dp71 is required to produce the abnormal ERG phenotype characterized by a delayed b-wave implicit time and a reduction of the b-wave amplitude (21). In the

Figure 5. Immunolocalization of Kir4.1 (C and D) and AQP4 (I and J) in vertical retinal sections from wild-type littermates (wt) and Dp71-null mice. Kir4.1 and AQP4 staining is distributed throughout the whole retina but strongly concentrated at the ILM and around the blood vessels (C and I, filled arrowheads). In Dp71-null retinae, Kir 4.1 and AQP4 staining is more diffuse; note the dramatic diminution of the labeling at the ILM and around the blood vessels for both Kir4.1 and AQP4 (D and J, open arrowheads) as compared with the wt (C and I, solid arrowheads). The vimentin immunolabel (used as a specific marker of Müller cells; A, B, G, H) and the merged images (E, F, K, L) show that Kir4.1 and AQP4 are localized in Müller cells. The changes in AQP4 immunolocalization are shown at higher magnification (M–R) in images taken with Nomarski optics (M, P) and with fluorescence recording (N, Q), as well as in the merged images (O, R); there is a clear shift from ILM- and blood vessel-associated expression in wild-type retinae (N, O) to a more diffuse pattern in retinae of Dp71-null mice (Q, R). Note that the reduced AQP4 immunofluorescence intensity at the ILM of the DP71-null retina is clearly visible in the fluorescence images (N versus Q) whereas the merged images (O versus R) emphasize the altered distribution pattern of the label. Scale bars (A–L and M–R), 25 μm.

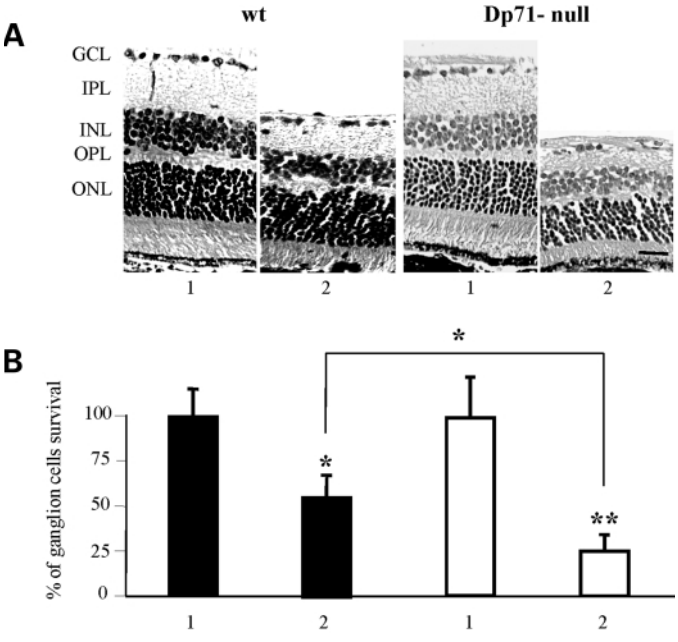

Figure 8. Ischemia/reperfusion-induced retinal changes in wild-type littermates (wt; n = 10) and Dp71-null mice (n = 10). Representative micrographs of hematoxylin and eosin stained 4 μm radial sections (A) and the mean of ganglion cell survival in non-ischemic (1) and ischemic (2) eyes of wt and Dp71-null mice (B). A slight decrease of the thickness of all layers as well as a strong diminution of the number of surviving ganglion cells, was observed in wt mice. These injuries were significantly increased in Dp71-null mice. Columns and error bars represent mean ± SEM (*$P < 0.05$;**$P < 0.01$). Scale bar, 25 μm.

mouse retina, the proteins dystrophin, Dp260 and Dp140 are found at the OPL where the highly specialized glutamatergic photoreceptor–bipolar cell–horizontal cell synapses are located. The dystrophin–DAPs, assembled as scaffold complexes at active zones of these synapses, may ensure the rapid and efficient release and reception of glutamate. It has already been excluded that this complex could be involved in the anchoring of the metabotropic glutamate receptor (mGluR6) in the post-synaptic ON bipolar cells, as the localization pattern of mGluR6 was not altered in mice lacking dystrophin, Dp260 and Dp140 (24). This suggests that the DMD gene products of the OPL may be involved in the presynaptic organization and anchoring of receptors and/or channels implicated in the b-wave generation; however, direct proofs of this hypothesis are lacking.

Our results support the current view that Müller cells are not directly involved in the generation of the b-wave since a virtually normal b-wave was recorded in Dp71-null mice (Fig. 1) despite a redistribution of the Kir4.1 channels in the Müller cell membrane (Fig. 6C and D), which should impair the K^+ current loops through the Müller cell processes (29). Nevertheless, it cannot be excluded that functional impairments occur in Müller cells of Dp71-null mice. We have shown here that Dp71 may be involved in scaffold complexes helping to anchor and/or localize other transmembraneous proteins that may modulate the electrical activity of the retina such as AQP4 (31), the glutamate transporter GLAST (55) or the nitric oxide synthase (56). Thus, the disruption of Dp71 might perturb ion and water fluxes through Müller cells that could affect the functioning of secondary and third-order neurons contributing to the generation of the b-wave (53,54). There might be other functional interactions between the DMD gene products located at the OPL (i.e. dystrophin, Dp260 and Dp140) and at the Müller cells (Dp71) contributing to b-wave generation, but this needs to be elucidated by further experiments. In this context, it may be of interest to note that an increased expression of utrophin in the Müller cells was found not only in Dp71 null-mice (present data) but also in mdx^{3cv} mice (40) characterized by a reduced b-wave. This argues against a possible direct physiological compensation of missing DMD gene products by upregulated utrophin expression, with respect to the ERG phenotype.

Furthermore, our ERG analysis revealed a slight diminution of the a-wave amplitude in the Dp71-null mice. Generally the a-wave is attributed solely to photoreceptor activity, although this has recently been questioned (57). We have shown that dystrophin, Dp260 and Dp140 are localized at the OPL; other studies have revealed the localization of full-length dystrophin and of Dp260 in the photoreceptor cells by immunoelectron microscopy or immunohistochemistry (58–61). In the Dp71-null mice studied here, Dp140 was found to be elevated (Fig. 2A). We cannot yet decide whether the decreased a-wave may directly be attributed to a change in the expression level of DMD gene products, or to an (unknown) indirect effect of the Müller cells on the photoreceptors.

Dystrophin-associated protein complexes

In the retina, β-dystroglycan is localized at the OPL, around the blood vessels and at the GCL/ILM; Müller cells express sarcoglycans; α1-syntrophin is distributed within the OPL and in Müller cells (40). We found that the absence of Dp71 resulted in a reduction of β-dystroglycan, specifically at the ILM and around the blood vessels, supporting the view that the localization of β-dystroglycan at the ILM is dependent upon the localization of Dp71, as previously proposed (34,43). Interestingly, the absence of Dp71 does not perturb the localization of other members of the dystrophin–glycoproteins complex (DGC), suggesting that a compensatory phenomenon may occur. Utrophin might be a candidate to play this role since it seems to be up-regulated in Dp71-null mice, and since it is exclusively expressed in the Müller cells (35).

Previous work on rat retinal Müller cells suggested the existence of a complex composed of Dp71 and/or utrophin, β-dystroglycan, δ-sarcoglycan, α-dystrobrevin and PSD-93. This complex could be involved in the clustering of transmembraneous proteins like the Kir4.1 potassium channel and the water channel AQP4 (36). Based upon these observations made on the mdx^{3cv} mouse model in which all the products of the DMD gene are greatly reduced but not entirely absent (40), it has been hypothesized that Dp71 could be critical for the clustered localization of the Kir4.1 channels (62). However, the involvement of other products of the DMD gene could not be ruled out. Moreover, it has been shown that dystrophin is responsible for an age-related reduction of AQP4 at the sarcolemmal level as well as in brain astrocytic end-feet at the capillaries of mdx mice (63). Our observation that the clustered localization of Kir4.1 and AQP4 around blood vessels and at the ILM was perturbed by the lack of Dp71 strongly

suggests that Dp71 is specifically involved in the patterning of Kir4.1 and AQP4 in Müller cells.

It has long been known from freeze-fracture studies that Müller cells display orthogonal arrays of intramembranous particles, highly concentrated at the endfoot region (64). Recently it was suggested that Kir4.1 and AQP4 (both integral membrane proteins) constitute parts of these arrays (28). It is tempting to speculate that also Dp71 and β-dystroglycan participate in the formation of functional arrays of Kir4.1 and AQP4 channels. However, since the two channels are differentially affected by the absence of Dp71, (a down-regulation occurred in the case of AQP4 but no changes were found for Kir4.1), it is possible that they are targeted and/or stabilized to the orthogonal arrays by different molecular mechanisms. This differential response to the absence of a product of the DMD gene is in agreement with previous observations for AQP4 in muscle and brain (63), and for Kir4.1 in retina (62). It is therefore likely that Kir4.1 and AQP4 might interact with the Dp71-β-dystroglycan complex via different DAPs. Thus, in Dp71-null retina the interaction of AQP4 with the complex may be insufficient for a stable retention in the membrane clusters, resulting in the degradation of the protein. Conversely in these mice the Kir4.1 interaction partners may stabilize the protein to the membrane but the targeting mechanism towards specific membrane compartments may be affected.

Ischemia-induced retinal damage in Dp71-null mice

In this study we show that Dp71 is not directly implicated in the generation of the b-wave of the ERG, but is involved in the stabilization of Kir4.1 channels and AQP4 water pores at specialized membrane areas of Müller glial cells. Furthermore, we observed an enhanced sensitivity against retinal ischemia-reperfusion in the Dp71-null mice. It is tempting to speculate of how the lack of Dp71 in Müller cells may increase the vulnerability of retinal ganglion cells under these conditions. The general ideas about the mechanisms of ischemic retinal ganglion cell death include the generation of free radicals, an accumulation of extracellular K^+, cell depolarization, enhanced glutamate release, enhanced Ca^{2+} influx, and, finally, apoptosis (65,66). In this context, it is important to note that one of the best-established functions of Müller cells is extracellular K^+ clearance or 'K^+ siphoning' (67,68). As we show here, an absence of Dp71 causes a re-distribution of Kir4.1 K^+ channels in the Müller cell membrane (Fig. 5). The normal accumulation of K^+ channels in the endfoot membrane is essential for retinal K^+ clearance, because Müller cells must 'eject' the excess K^+ ions into the vitreous body (and into blood vessels, in vascularized retinae) (67–69). Thus, in the Dp71-null mice where a lack of K^+ channels occurs in the Müller cell endfoot membrane, any ischemia-induced extracellular K^+ accumulation (e.g. due to lack of energy to maintain Na,K pump activity and/or to Na,K pump inhibition) cannot be siphoned into the vitreous, and must cause enhanced depolarization, glutamate release, Ca^{2+} influx and death of ganglion cells. The situation is likely to be worsened by the fact that elevated extracellular K^+ levels depolarize the cells, and, thus, impair the activity of the glial glutamate uptake carriers which are electrogenic (55). The down-regulation and displacement of AQP4 may also participate in the molecular mechanisms causing an enhanced vulnerability of ganglion cells to transient ischemia. In particular, it is feasible that retinal edema may be involved in the degenerative processes, and may be enhanced by a disturbed function of AQP4.

In summary, the findings reported here clearly reveal that Dp71 is required for the proper localization of Kir4.1 and AQP4 channels in the membrane of Müller cells. We also provide evidence for functional retinal deficits associated with the lack of Dp71.

MATERIALS AND METHODS

Animals

The Dp71-null strain was obtained by replacing via homologous recombination most of the first and unique exon of Dp71 and of a small part of the Dp71 first intron with a sequence encoding a β-gal-neomycine-resistance chimeric protein (β-geo) (33). This abolished the expression of Dp71 without interfering with the expression of other products of the DMD gene. Mice were identified by analysis of PCR products using the following oligonucleotide primers (Dp71F, ATGAGGGAACAGCTCAAAGG; Dp71R, TGCAGCTGACAGGCTCAAGA). Control immunoblot experiments were also performed in brain slices to verify the Dp71-null phenotype (unpublished data). The animals were bred in our laboratory and their littermates were used as controls for the study. All experiments were done in compliance with the European Communities Council Directives (86/609/EEC) for animal care and experimentation.

ERG

Ganzfeld ERGs were recorded from dark-adapted animals, anesthetized by an intraperitoneal injection of a mixture of hypnovel (2.5 mg/ml) and hypnomidate (0.4 mg/ml) (1:1). The pupil of the right eye was dilated with a drop of 0.5% tropicamide (2 mg/0.4 ml) and the cornea was anesthetized with a drop of oxybuprocaine chlorhydrate (1.6 mg/0.4 ml). Responses were recorded from the cornea using a gold electrode; ground and reference needle-electrodes were inserted subcutaneously on the head. A stimulator mounted in a Ganzfeld dome produced an integrated white-light value of 10 cd/m^2 at the plane of the eye. Ten responses separated in their representation by 60 s were averaged using a band-pass frequency of 0.1–1000 Hz. Data were digitized using the Multiliner Vision Program (Toennies, Germany). The implicit time of the a-wave (a negative potential reflecting the hyperpolarizing photoreceptor light response) and the b-wave (a positive potential reflecting contributions of bipolar, amacrine and/or Müller cells) was defined as the duration between the rise of the stimulus and the peak of the waves. The b-wave amplitude was determined from the bottom of the a-wave to the top of the b-wave. ERG measurements were analyzed by Student's t-test using Prism logiciel.

X-gal staining

Eyes from 1 to 3-month-old mice were either treated directly for whole-mount X-gal staining, or embedded in O.C.T

compound and frozen in liquid nitrogen. For whole-mount staining, the eyes were washed with phosphate-buffered saline (PBS), fixed for about 1 h in 4% paraformaldehyde (PFA), and stained overnight with X-gal (70). Sodium desoxycholate (0.01%) and NP-40 (0.02%) were added to the staining buffer. The stained eyes were post-fixed overnight in 4% PFA, dehydrated, embedded in paraffin and cut on a microtome. The slices were deparafinized with xylene (2 min), rehydrated (from 95 to 25% ethanol), counterstained with nuclear fast red (3 min), dehydrated again and mounted with entellan. The frozen eyes were first cut on a cryostat (10–15 μm) and then stained with X-gal, counterstained and mounted as described above.

Electrophoresis, western blotting and immunodetection

Murine retinae were homogenized at 4°C in 10 vols (wt/vol) extraction buffer. Protein concentrations were evaluated by quantitative Coomassie stain (71). Protein extracts were resolved on 7% gradient polyacrylamide-SDS gels. They were then electrotransferred to Schleicher and Schuell nitrocellulose membranes (Dassel, Germany) (72). Blots were blocked with 1% bovine serum albumin (BSA) and 3% dry milk (BIO-RAD, Herts, UK) in PBS for 1 h, then incubated with either primary antibody for 120 min at room temperature. After washing, they were probed with a HRP labeled goat anti-rabbit secondary antibody (Interchim, France). Chemiluminescence detection was finally performed using a ECL+ plus western blotting detection system (Amersham Biosciences, UK).

Tissue preparation and immunohistochemistry

After enucleation, the eyes of mice were embedded in OCT compound, and frozen in liquid nitrogen. They were vertically sliced at 7 μm thickness in a cryostat and placed on gelatin-coated slide glasses. The cryosections were fixed with 4% PFA for 4 min and rinsed three times with PBS. The sections were blocked and permeabilized with 0.1% Triton, 0.1% BSA diluted in PBS for 15 min. They were incubated with primary antibodies, diluted in PBS, 0.5% BSA for 120 min. Following this incubation, the sections were washed three times with PBS. Secondary antibodies (Interchim, France) coupled to Alexa were used, diluted 1 : 500 in PBS, 0.5% BSA. Then the sections were rinsed three times with PBS, 0.5% BSA. Cell nuclei were stained using DAPI, 1 : 200 in PBS, 0.5 % BSA (Molecular Probes, Eugene, OR, USA). Sections were examined on a fluorescence microscope (×40 objectives; Optiphot 2, Nikon, Tokyo, Japan), and/or on a confocal laser-scanning microscope (LSM 510, Zeiss, Germany).

Antibodies

The antibodies directed against dystrophin gene products Dys2 and 2166 have been previously described (40,37). K7 is a rabbit polyclonal antibody directed against a synthetic peptide CPNVPSRPQAM-COOH corresponding to the C-terminal end of utrophin. 2166 was kindly provided by D. Blake (UK). Antibodies against dystrophin-associated glycoprotein complex; JAF (β-dystroglycan), Nini (δ-Sarcoglycan), PEP1 (γ-sarcoglycan) and C4 (α1-syntrophin) were previously characterized (73). Polyclonal anti-aquaporin-4 AQP4 was from Chemicon (CA, USA) and anti-inwardly rectifying potassium channel (Kir4.1) is a polyclonal antibody raised in rabbit from Alomone labs (Israel) and mouse monoclonal anti-actin was from Chemicon international (CA, USA). RetG7 is a monoclonal antibody raised against vimentin kindly provided by D. Hicks.

Electrophysiology on isolated Müller cells (patch-clamp)

For electrophysiological recordings, Müller cells were freshly isolated from murine retina. For this purpose, retinal tissue was stored for 30 min in Ca^{2+}/Mg^{2+}-free PBS containing 0.2–0.4 mg/ml papain (Boehringer, Mannheim, Germany) at 37°C. After washing with PBS containing DNase I (160 U/ml; Sigma, Deisenhofen, Germany), the retina was triturated using a 1 ml pipette tip until single Müller cells were dissociated. Isolated cells were stored until use in minimum essential medium (Sigma, Deisenhofen, Germany) on ice. Recordings were performed in the whole-cell configuration of the patch-clamp technique (74). Cells were suspended in extracellular solution in a recording chamber mounted on the stage of a microscope (Axioskop, Zeiss, Germany) where they settled down. Control extracellular solution contained (mM): NaCl, 110; KCl, 3; $CaCl_2$, 2; $MgCl_2$, 1; Na_2HPO_4, 1; glucose, 10; HEPES–Tris, 10; $NaHCO_3$, 25. It was equilibrated to pH 7.4 by continuously bubbling with carbogen gas (95% O_2, 5% CO_2) during continuous perfusion at 2 ml/min. Experiments were performed at room temperature (20–24°C). Recording electrodes were made from borosilicate glass (Science Products, Hofheim, Germany) and had resistances of 4–6 MΩ when filled with an intracellular solution containing (mM): KCl, 130; NaCl, 10; $MgCl_2$, 2; $CaCl_2$, 1; EGTA, 10; HEPES–Tris, 10; pH 7.1.

Recordings were carried out using the patch clamp amplifier Axopatch 200A (Axon Instruments, Foster City, CA, USA). Currents were low-pass filtered at 1 kHz with an eight-pole Bessel filter and digitized at 5 kHz using a 12 bit-A/D converter. Voltage command protocols were generated and data analysis was performed with the software ISO 2 (MFK, Niedernhausen, Germany). The 'resting membrane potential' (zero current potential) was recorded in the current clamp mode.

Induction of transient retinal ischemia

Adult mice (7–10 weeks old) were anaesthetized with intraperitoneal injections of pentobarbital (60 mg/kg). The pupils were dilated with 1% tropicamide and corneal analgesia was achieved with 1 drop of Neosynephrine 10%. Retinal ischemia was induced for 60 min by introducing a 32-gage needle into the anterior chamber (using a micromanipulator) of the left eye, in order to increase the pressure up to 150 mmHg (75) while the right eye served as non-ischemic control. The animals were sacrificed 14 days after reperfusion, and the eyes were enucleated for histological and morphometric studies.

Histology and morphometry

The enucleated eyes were fixed in 4% paraformaldehyde and embedded in paraffin. The posterior part of the eyes was sectioned sagittally at 4 μm thickness through the optic nerve, mounted and stained with hematoxylin and eosin. For the estimation of the number of ganglion cells, counting was performed with optiscan and optilab software. Four sections of each eye were used for measurements. Ten animals were used in each group. Results are presented as mean ± SEM. The nonparametric ANOVA test was used to estimate the significance of the results.

ACKNOWLEDGEMENTS

We thank Gérald Hugon and Nicolas Lethenet for technical assistance respectively in antibody preparation and animal care and also D. Blake and D. Hicks for the 2166 and Ret G7 antibodies. This work was supported by INSERM (Institut National de la Santé Et de la Recherche Médicale) and by grants from the AFM (Association Française contre les Myopathies) to A.R., D.Y., U.N. and D.M.; from MDA (USA), GIF, and ISF to U.N. and D.Y.; and from the Bundesministerium für Bildung, Forschung und Technologie (BMB+F), interdisciplinary Center for Clinical Research at the University of Leipzig (01KS9504, Project C5) to A.R. C.D. received financial support from ADRET Alsace (Association pour l'Aide au Développement de la Recherche sur la Régénération de la Rétine et sa Transplantation), FAF (Fédération des Aveugles et handicapés visuels de France) and the AFM. P.F. and A.B. received financial support respectively from the FAF and Retina France.

REFERENCES

1. Koenig, M., Monaco, A.P. and Kunkel, L.M. (1988) The complete sequence of dystrophin predicts a rod-shaped cytoskeletal protein. Cell, 53, 219–226.
2. Matsumura, K. and Campbell, K.P. (1994) Dystrophin-glycoprotein complex: its role in the molecular pathogenesis of muscular dystrophies. Muscle Nerve, 17, 2–15.
3. Suzuki, A., Yoshida, M., Hayashi, K., Mizuno, Y., Hagiwara, Y. and Ozawa, E. (1994) Molecular organization at the glycoprotein-complex binding site of dystrophin. Three dystrophin-associated proteins bind directly to the carboxy-terminal portion of dystrophin. Eur. J. Biochem., 220, 283–292.
4. Henry, M.D. and Campbell, K.P. (1996) Dystroglycan: an extracellular matrix receptor linked to the cytoskeleton. Curr. Opin. Cell. Biol., 5, 625–631.
5. Gilgenkrantz, H. and Cartaud, J. (1998) All you want to know about the neuromuscular junction. Med. Sci., 14, 230–233.
6. Thomas, G.D., Sander, M., Lau, K.S., Huang, P.L., Stull, J.T. and Victor, R.G. (1998) Impaired metabolic modulation of alpha-adrenergic vasoconstriction in dystrophin-deficient skeletal muscle. Proc. Natl Acad. Sci. USA, 95, 15090–15095.
7. Liu, J.W., Wakayama, Y., Inoue, Shibuya, S., Kojima, H., Jimi, T. and Oniki, H. (1999) Immunocytochemical studies of aquaporin 4 in the skeletal muscle of mdx mouse. J. Neurol. Sci., 164, 24–28.
8. Emery, A.E. (1993) Duchenne Muscular Dystrophy. Oxford University Press, New York.
9. Zubrzycka-Gaarn, E.E., Bulman, D.E., Karpati, G., Burghes, A.H., Belfall, B., Klamut, H.J., Talbot, J., Hodges, R.S., Ray, P.N. and Worton, R.G. (1988) The Duchenne muscular dystrophy gene product is localized in sarcolemma of human skeletal muscle. Nature, 333, 466–469.
10. Nudel, U., Robzyk, K. and Yaffe, D. (1988) Expression of the putative Duchenne muscular dystrophy gene in differentiated myogenic cell cultures and in the brain. Nature, 331, 635–638.
11. D'Souza, V.N., Man, N., Morris, G.E., Karges, W., Pillers, D.A. and Ray, P.N. (1995) A novel dystrophin isoform is required for normal retinal electrophysiology. Hum. Mol. Genet., 4, 837–842.
12. Lidov, H.G.W., Selig, S. and Kunkel, L.M. (1995) Dp140: a novel 140 kDa CNS transcript from the dystrophin locus. Hum. Mol. Genet., 4, 329–335.
13. Byers, T., Lidov, H. and Kunkel, L. (1993) An alternative dystrophin transcript specific to peripheral nerve. Nat. Genet., 4, 77–81.
14. Bar, S., Barnea, E., Levy, Z., Neuman, S., Yaffe, D. and Nudel, U. (1990) A novel product of the Duchenne muscular dystrophy gene which greatly differs from the known isoforms in its structure and tissue distribution. Biochem. J., 272, 557–560.
15. Blake, D.J., Love, D.R., Tinsley, J., Morris, G.E., Turley, H., Gatter, K., Dickson, G., Edwards, Y.H. and Davies, K.E., (1992) Characterization of a 4.8 kb transcript from the Duchenne muscular dystrophy locus expressed in Schwannoma cells. Hum. Mol. Genet., 1, 103–109.
16. Hugnot, J.P., Gilgenkrantz, H., Vincent, N., Chafey, P., Morris, G.E., Monaco, A.P., Berwald-Netter, Y., Koulakoff, A., Kaplan, J.C., Kahn, A. et al. (1992) Distal transcript of the dystrophin gene initiated from an alternative first exon and encoding a 75-kDa protein widely distributed in nonmuscle tissues. Proc. Natl Acad. Sci. USA, 89, 7506–7510.
17. Lidov, H.G. (1996) Dystrophins in the nervous system. Brain Pathol., 6, 63–77.
18. Schmitz, F. and Drenckhahn, D. (1997) Dystrophin in the retina. Prog. Neurobiol., 53, 547–560.
19. Claudepierre, T., Rodius, F., Frasson, M., Fontaine, V., Picaud, S., Dreyfus, H., Mornet, D. and Rendon, A. (1999) Differential distribution of dystrophins in rat retina. Invest. Ophthal. Visual Sci., 40, 1520–1529.
20. Sigesmund, D.A., Weleber, R.G., Pillers, D.M., Westall, C.A., Panton, C.M., Powell, B.R., Heon, E., Murphey, W.H., Musarella, M.A. and Ray, P.N. (1994) Characterization of the ocular phenotype of Duchenne and Becker muscular dystrophy. Ophthalmology, 101, 856–865.
21. Pillers, D.M., Weleber, R.G., Woodward, W.R., Green, D.G., Chapman, V.M. and Ray, P.N. (1995) mdx^{3cv} Mouse is a model for electroretinography of Duchenne/Becker muscular dystrophy. Invest. Ophthal. Visual Sci., 36, 462–466.
22. Pillers, D.M., Bulman, D.E., Weleber, R.G., Sigesmund, D.A., Musarella, M.A., Powell, B.R., Murphey, W.H., Westall, C.A., Panton, C.M., Becker, L.E., Worton, R.G. and Ray, P.N. (1993) Dystrophin expression in the human retina is required for normal function as defined by electroretinography. Nat. Genet., 4, 82–86.
23. Cibis, G.W., Fitzgerald, K.M., Harris, D.J., Rothberg, P.J. and Rupani, M. (1993) The effects of dystrophin gene mutations on the ERG in mice and humans. Invest. Ophtal. Visual Sci., 34, 3646–3652.
24. Kameya, S., Araki, E., Katsuki, M., Mizota, A., Adachi, E., Nakahara, K., Nonaka, I., Sakuragi, S., Takeda, S. and Nabeshima, Y. (1997) Dp260 disrupted mice revealed prolonged implicit time of the b-wave in ERG and loss of accumulation of beta-dystroglycan in the outer plexiform layer of the retina. Hum. Mol. Genet., 6, 2195–2203.
25. Pillers, D.M., Fitzgerald, K.M., Duncan, N.M., Dwinnell, S.J., Rash, S.M., White, R.A., Powell, B.R., Schnur, R.E., Ray, P.N., Cibis, G.W. and Weleber, R.G. (1999) Duchenne/Becker muscular dystrophy: Correlation of phenotype by electroretinography with sites of dystrophin mutations. Hum. Genet., 105, 2–9.
26. Pillers, D.M., Weleber, R.G., Green, D.G., Rash, S.M., Dally, G.Y., Howard, P.L., Powers, M.R., Hood, D.C., Chapman, V.M., Ray, P.N. and Woodward, R. (1999) Effects of dystrophin isoforms on signal transduction through neural retina: genotype–phenotype analysis of Duchenne Muscular Dystrophy mouse mutants. Mol. Genet. Metab., 66, 100–110.
27. Fitzgerald, K.M., Cibis, G.W., Gettel, A.H., Rinaldi, R., Harris, D.J. and White, R.A. (1999) ERG phenotype of a dystrophin mutation in heterozygous female carriers of Duchenne muscular dystrophy. J. Med. Genet., 36, 316–322.
28. Nagelhus, E.A., Horio, Y., Inanobe, A., Fujita, A., Haug, F.M., Nielsen, S., Kurachi, Y. and Ottersen, O.P. (1999) Immunogold evidence suggests that coupling of K+ siphoning and water transport in rat retinal Müller cells is mediated by a coenrichment of Kir 4.1 and AQP4 in specific membrane domains. Glia, 26, 47–54.
29. Newman, E.A. and Odette, L.L. (1984) Model of electroretinogram b-wave generation: a test of the K+ hypothesis. J. Neurophysiol., 51, 164–182.

30. Kofuji, P., Ceelen, P., Zahs, K.R., Surbeck, L.W., Lester, H.A. and Newman, E.A. (2000) Genetic inactivation of an inwardly rectifying potassium channel (Kir 4.1 subunit) in mice: phenotypic impact in retina. J. Neurosci., 20, 5733–5740.
31. Li, J., Patil, R.V. and Verkman, A.S. (2002) Mildly abnormal retinal function in transgenic mice without Müller cell aquaporin-4 water channels. Invest. Ophthal. Visual Sci., 43, 573–579.
32. Lederfein, D., Levy, Z., Augier, N., Mornet, D., Morris, G., Fuchs, O., Yaffe, D. and Nudel, U. (1992) A 71-kDa protein is the major product of the Duchenne muscular dystrophy gene in brain and other non-muscle tissues. Proc. Natl Acad. Sci. USA, 89, 5346–5350.
33. Sarig, R., Metger-Lallemand, V., Gitelman, I., Davis, C., Fuchs, O., Yaffe, D. and Nudel, U. (1999) Targeted inactivation of Dp71, the major non-muscle product of the DMD gene: differential activity of the Dp71 promoter during development. Hum. Mol. Genet., 8, 1–10.
34. Howard, P.L., Ghassan, Y.D., Wong, M.H., Ho, A., Weleber, R.G., Pillers, D.M. and Ray, P.N. (1998) Localization of dystrophin isoform Dp71 to the inner limiting membrane of the retina suggests a unique functional contribution of Dp71 in the retina. Hum. Mol. Genet., 7, 1385–1391.
35. Claudepierre, T., Mornet, D., Pannicke, T., Forster, V., Dalloz, C., Bolanõs-Jimenez, F., Sahel, J., Reichenbach, A. and Rendon, A. (2000) Expression of Dp71 in Müller glial cells: a comparison with utrophin and dystrophin associated proteins. Invest. Ophthal. Visual Sci., 41, 294–304.
36. Claudepierre, T., Dalloz, C., Mornet, D., Matsumura, K., Sahel, J. and Rendon, A. (2000) Characterization of the intramolecular associations of the dystrophin-associated glycoproteins complex in retinal Müller glial cells. J. Cell Sci., 113, 3409–3417.
37. Blake, D.J., Hawkes, R., Benson, M.A. and Beesley, P.W. (1999) Different dystrophin-like complexes are expressed in neurons and glia. J. Cell. Biol., 147, 645–657.
38. Mizuno, Y., Yoshida, M., Nonaka, I., Hirai, S. and Ozawa, E. (1994) Expression of utrophin (dystrophin-related protein) and dystrophin-associated glycoproteins in muscles from patients with Duchenne muscular dystrophy. Muscle Nerve, 17, 206–216.
39. Greenberg, D.S., Schatz, Y., Levy, Z., Pizzo, P., Yaffe, D. and Nudel, U. (1996) Reduced levels of dystrophin associated proteins in the brains of mice deficient for Dp71. Hum. Mol. Genet., 5, 1299–1303.
40. Dalloz, C., Claudepierre, T., Rodius, F., Mornet, D., Sahel, J. and Rendon, A. (2001) Differential distribution of the members of dystrophin glycoprotein complex in mouse retina: effect of the mdx3cv mutation. Mol. Cell. Neurosci., 17, 908–920.
41. Montanaro, F., Carbonetto, S., Campbell, K.P. and Lindenbaum, M. (1995) Dystroglycan expression in the wild-type and mdx mouse neural retina: synaptic colocalization with dystrophin, dystrophin-related protein but not laminin. J. Neurosci. Res., 42, 528–538.
42. Ueda, H., Gohdo, T. and Ohno, S. (1998) Beta-dystroglycan localization in the photoreceptor and Müller cells in the rat retina revealed by immunoelectron microscopy. J. Histochem. Cytochem., 46, 185–191.
43. Blank, M., Koulen, P., Blake, D.J. and Kroger, S. (1999) Dystrophin and beta-dystroglycan in photoreceptor terminals from normal and mdx3cv mouse retinae. Eur. J. Neurosci., 11, 2121–2133.
44. Distler, C., Bronzel, M., Paas, I. and Wahle, P. (1997) Biochemical and histological analysis of two Muller cell antibodies in developing and adult cat and rat central nervous system. Cell Tissue Res., 289, 411–426.
45. Bringmann, A., Francke, M., Pannicke, T., Biedermann, B., Kodal, H., Faude, F., Reichelt, W. and Reichenbach, A. (2000) Role of glial K^+ channels in ontogeny and gliosis: a hypothesis based upon sudies on Müller cells. Glia, 29, 35–44.
46. Hashimoto, J., Murakami, M. and Tomita, T. (1961) Localization of the ERG by aid of histological method. Jap. J. Physiol., 11, 62–70.
47. De Becker, I., Riddell, D.C., Dooley, J.M. and Tremblay, F. (1994) Correlation between electroretinogram findings and molecular analysis in the Duchenne muscular dystrophy. Br. J. Ophthal., 78, 719–722.
48. Jensen, H., Warburg, M., Sjo, O. and Schwartz, M. (1996) Duchenne muscular dystrophy: negative electroretinograms and normal dark adaptation. Reappraisal of assignment of X linked incomplete congenital stationary night blindness. J. Med. Genet., 32, 348–351.
49. Miller, R.F. and Dowling, J.E. (1970) Intracellular responses of the Müller (Glial) cells of mudpuppy retina: their relation to b-wave of the electroretinogram. J. Neurophysiol., 33, 323–342.
50. Newman, E.A. (1980) Current source-density analysis of the b-wave of frog retina. J. Neurophysiol., 43, 1355–1366.
51. Stockton, R.A. and Slaughter, M.M. (1989) b-Wave of the electroretinogram. A reflection of ON bipolar cell activity. J. Gen. Physiol., 93, 101–122.
52. Hanitzsch, R., Lichtenberger, T. and Mättig, W.-U. (1996) The influence of $MgCl_2$ and APB on the light-induced potassium changes and the ERG b-wave of the isolated superfused rat retina. Vision Res., 36, 499–507.
53. Wurziger, K., Lichtenberger, T. and Hanitzsch, R. (2001) On-bipolar cells and depolarising third-order neurons as the origin of the ERG-b-wave in the RCS rat. Vision Res., 20, 1091–1101.
54. Dong, C.J. and Hare, W.A. (2000) Contribution of the kinetics and amplitude of the electroretinogram b-wave by third-order retinal neurons in the rabbit retina. Vision Res., 40, 579–589.
55. Harada, T., Harada, C., Watanabe, M., Inoue, Y., Sakagawa, T., Nakayama, N., Sasaki, S., Okuyama, S., Watase, K., Wada, K. and Tanaka, K. (1998) Functions of the two glutamate transporters GLAST and GLT-1 in the retina. Proc. Natl Acad. Sci. USA, 95, 4663–4666.
56. Adams, M.E., Mueller, H.A. and Froehner, S.C. (2001) In vivo requirement of the alpha-syntrophin PDZ domain for the sarcolemmal localization of nNOS and aquaporin-4. J. Cell Biol., 155, 113–122.
57. Bush, A.L. and Sieving, P.A. (1994) A proximal retinal component in the primate photopic ERG a-wave. Invest. Ophthal. Visual Sci., 35, 635–645.
58. Miike, T., Miyatake, M., Zhao, J., Yoshioka, K. and Uchino, M. (1989) Immunohistochemical dystrophin reaction in synaptic regions. Brain Dev., 11, 344–346.
59. Schmitz, F., Holbach, M. and Drenckhahn, D. (1993) Colocalization of retinal dystrophin and actin postsynaptic dendrites of rod and cone photoreceptor synapses. Histochemistry, 100, 473–479.
60. Ueda, H., Kobayashi, T., Mitsui, K., Tsurugi, K., Tsukahara, S. and Ohno, S. (1995) Dystrophin localization at presynapse in rat retina revealed by immunoelectron microscopy. Invest. Ophthal. Visual Sci., 36, 2318–2332.
61. Ueda, H., Baba, T., Terada, N., Kato, Y., Tsukahara, S. and Ohno, S. (1997) Dystrophin in rod spherules: submembranous dense regions facing bipolar cell processes. Histochem. Cell Biol., 108, 243–248.
62. Connors, N.C. and Kofuji, P. (2002) Dystrophin Dp71 is critical for the clustered localization of potassium channels in retinal glial cells. J. Neurosci., 22, 4321–4327.
63. Frigeri, A., Nicchia, G.P., Nico, B., Quondamatteo, F., Herken, R., Roncali, L. and Svelto, M. (2001) Aquaporin-4 deficiency in skeletal muscle and brain of dystrophic mdx mice. FASEB J., 15, 90–98.
64. Wolburg, H. (1995) Orthogonal arrays of intramembranous particles: a review with special reference to astrocytes. J. Hirnforsch., 36, 239–256.
65. Bonne, C., Müller, A. and Villain, M. (1998) Free radicals in retinal ischemia. Gen. Pharmac., 30, 275–280.
66. Sucher, N.J., Lipton, S.A. and Dreyer, E.B. (1997) Molecular basis of glutamate toxicity in retial ganglion cells. Vision Res., 37, 3483–3493.
67. Newman, E.A. (1984) Regional specialization of retinal glial cell membrane. Nature, 309, 155–157.
68. Karwoski, C.J., Lu, H.-K. and Newman, E.A. (1989) Spatial buffering of retinal light-evoked potassium increases by retinal Müller (glial) cells. Science, 244, 578–580.
69. Kofuji, P., Biedermann, B., Siddharthan, V., Raap, M., Iandiev, I., Milenkovic, I., Thomzig, A., Veh, R.W., Bringmann, A. and Reichenbach, A. (2002) Kir potassium channel subunit expression in retinal glial cells: implications for spatial potassium buffering. Glia, 39, 292–303.
70. Lallemand, Y. and Brulet, P. (1990) An in situ assessment of the routes and extents of colonisation of the mouse embryo by embryonic stem cells and their descendants. Development, 110, 1241–1248.
71. Esen, A. (1978) A simple method for quantitative, semiquantitative, and qualitative assay of protein. Anal. Biochem., 89, 264–273.
72. Towbin, H., Staehelin, T. and Gordon, J. (1979) Electrophoretic transfer of proteins from polyacrilamide gels to nitrocellulose sheets: procedure and some applications. Proc. Natl Acad. Sci. USA, 76, 4350–4354.
73. Rivier, F., Robert, A., Hugon, G., Bonet-Kerrache, A., Nigro, V., Fehrentz, J.A., Martinez, J. and Mornet, D. (1999) Dystrophin and utrophin complexed with different associated proteins in cardiac Purkinje fibres. Histochem. J., 31, 425–432.
74. Hamill, O.P., Marty, A., Neher, E., Sakmann, B. and Sigworth, J. (1981) Improved patch-clamp techniques for high-resolution current recording from cells and cell-free membrane patches. Pflügers Archiv., 391, 85–100.
75. Kroll, A.J. (1968) Experimental central retinal artery occlusion. Arch. Ophthal., 79, 453–469.